

Diode laser slit-jet spectra and analysis of the ν_7 fundamental of 1-chloro-1,1-difluoroethane (HCFC-142b)

M. Snels¹ and G. D'Amico^{2,a}

¹ Istituto di Scienze dell'Atmosfera e del Clima, Sezione di Roma, CNR, Via Fosso del Cavaliere 100, 00133 Roma, Italy

² Istituto di Metodologie Inorganiche e dei Plasmi, Sezione di Potenza, CNR, Zona Industriale, 85050 Tito Scalo (PZ), Italy

Received 20 May 2002 / Received in final form 10 July 2002

Published online 24 September 2002 – © EDP Sciences, Società Italiana di Fisica, Springer-Verlag 2002

Abstract. High resolution infrared spectra (0.001 cm^{-1}) have been measured for mixtures of 1-chloro-1,1-difluoroethane in Ne, expanded in a supersonic planar jet. The ν_7 fundamental has been analyzed for both isotopic species, $\text{CH}_3\text{CF}_2^{35}\text{Cl}$ and $\text{CH}_3\text{CF}_2^{37}\text{Cl}$. A weak *b*-type component has been observed for the first time.

PACS. 33.20.Vq Vibration-rotation analysis – 39.10.+j Atomic and molecular beam sources and techniques – 92.70.Cp Atmosphere

1 Introduction

Hydrochlorofluorocarbons (HCFC's) have been introduced worldwide in order to substitute the well-known chlorofluorocarbons (CFC's), whose production has been gradually reduced since the ratification of the Montreal protocol by most industrial countries in 1987. As a result of the application of the Montreal protocol and its amendments (London, 1990 and Copenhagen, 1992), the stratospheric abundance of some CFC's is declining since the last few years. Montzka *et al.* [1] observed a decrease of the global tropospheric abundance of Cl in 1995 of 25 ± 5 ppt per year and predicted that the amount of reactive chlorine and bromine would reach a maximum in the stratosphere between 1997 and 1999 and decline thereafter. In the last decades alternative compounds, including the HCFC's, have been developed to replace CFC's in applications such as refrigeration, foam blowing, insulation, electronic cleaning and drying. The ozone depletion potential of these HCFC's is supposed to be significantly less than that of the CFC's, due to their more efficient reaction with the hydroxyl radical in the troposphere. The atmospheric lifetime of the HCFC's is thus appreciably shorter (about 20 years for CFC-142b [2]) than that of CFC-11 (50 years) and CFC-12 (100 years).

The potential contribution of the CFC's and their replacements (HCFC's, among others), being strong infrared absorbers, to the greenhouse effect has to be considered as well. The global warming potential of some

HCFC's is comparable to or even higher than that of the CFC's [3]. Since their introduction, the global mixing ratios for the HCFC's are steadily increasing, although they are much lower than those of the CFC's. For HCFC-142b and HCFC-141b global mixing ratios of 4.3 ppt and 0.7 ppt respectively have been measured [4] in 1993, with an increase rate of 1.1 ppt and 0.9 ppt per year.

Infra red spectroscopy is a powerful tool for monitoring trace gases in the atmosphere and spectroscopic investigations of the most important HCFC's are required for supporting the detection and quantification of HCFC's in the atmosphere. Many of the available data concerning the chlorofluorocarbon concentrations in the stratosphere have been obtained by analyzing high resolution Fourier transform solar transmission spectra. The ATMOS (Atmospheric Trace Molecule Spectroscopy) experiment was designed for stratospheric observations from the space shuttle [5,6]. Both ATMOS and MarkIV [7] (a balloon operated FTIR instrument) produced high resolution (0.01 cm^{-1}) limb-viewing spectra which were analyzed by using empirical line files, which were fitted to laboratory spectra. The uncertainty resulting from the use of empirical spectroscopic parameters is estimated to be about $\pm 25\%$, excluding systematic errors [6]. The availability of accurate molecular parameters would improve the retrieval procedures both for high as for medium resolution trace gas spectra. An interesting example is the case of the ν_4 fundamental of CCl_3F which produces a strong absorption band at about 850 cm^{-1} , which has been observed in limb spectra but also in nadir-looking devices on satellites. This band shows a rather shapeless absorption at low wavenumbers and very pronounced features at the higher wavenumbers, and was not understood until

^a Also: Dipartimento di Scienze Fisiche Università di Napoli "Federico II" Complesso Universitario di M.S. Angelo, 80126 Napoli, Italy.

e-mail: m.snels@isac.cnr.it

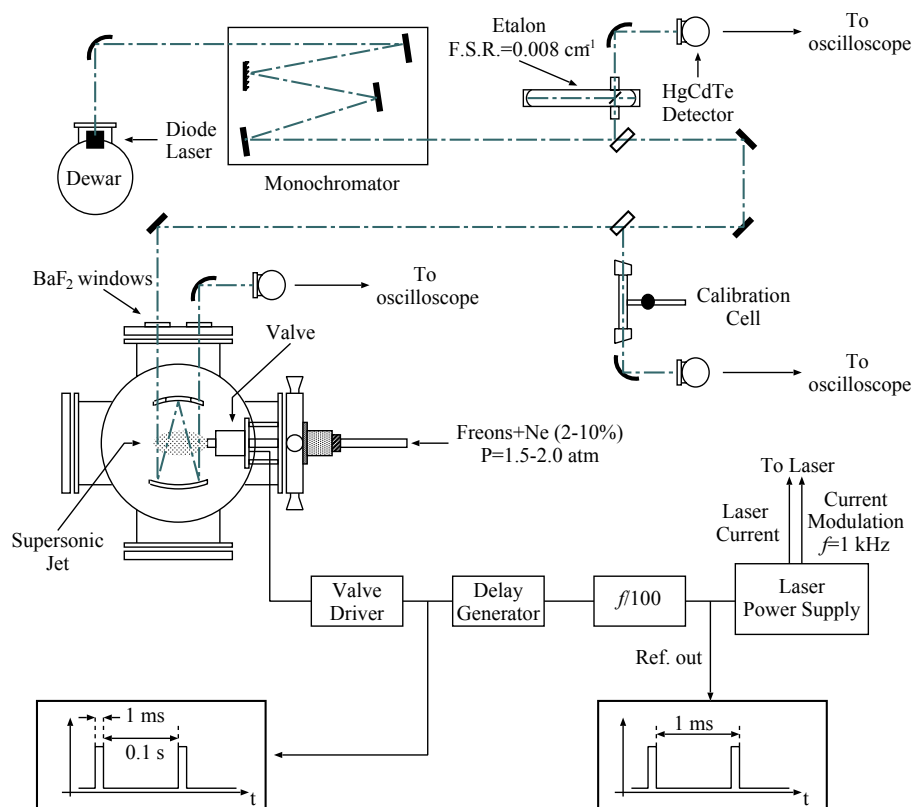


Fig. 1. Experimental set-up. The optical path of the diode laser radiation is indicated by a dash-dot line. In the lower part of the figure the timing circuit which synchronizes the laser scan with the pulsed valve is shown.

the analysis of a high resolution slit-jet diode laser spectrum [10] shed light on this problem and provided accurate molecular parameters which describe both high and low resolution spectra excellently.

The infrared absorption spectra of CFC's and HCFC's are often rather complex, due to the high line density and the limited instrumental resolution. The presence of hot-bands and different chlorine isotopic species renders the analysis even more troublesome. We have previously demonstrated [8–12] that the diode laser slit-jet technique, which combines high resolution (0.001 cm^{-1} FWHM typically) with low rotational and vibrational temperatures, can simplify the spectra enormously, allowing for unambiguous assignments and successful analyses. Here the analysis of the ν_7 band of CFC-142b is presented, showing the potential of this method, permitting a straightforward assignment of well resolved lines for both isotopic species, $\text{CH}_3\text{CF}_2^{35}\text{Cl}$ and $\text{CH}_3\text{CF}_2^{37}\text{Cl}$.

2 Experimental details

The advantages of slit jet spectroscopy have been recognized since many years and both CW mode [13,14] and pulsed [15–18] slit jets have been used to obtain narrow absorption lines due to velocity quenching parallel to the slit. All measurements reported here have been taken with our slit jet diode laser apparatus (see Fig. 1 for details), consisting of a liquid nitrogen cooled Dewar containing up to four diode lasers, a mode selecting monochromator, an internally coupled confocal etalon and a pulsed molecular

jet. The radiation emitted by a multimode diode laser was collimated with an off-axis parabolic mirror and mode filtered by a 0.5 m focal length monochromator. A small part of the radiation was used for calibration purposes, while the main laser beam was directed into a vacuum chamber equipped with BaF_2 windows and evacuated by a 3000 l/s oil diffusion pump backed by a $60 \text{ m}^3/\text{h}$ two stage rotary pump. Compact White cell optics (about 15 cm basic length) was employed for multiple passing the laser beam through the supersonic jet expansion. With a careful alignment procedure it was possible to obtain about 15 passes through an area of $2 \times 2 \text{ mm}$. Eventually the out coming laser beam was focused onto a HgCdTe detector with an off-axis parabolic mirror. A pulsed valve, model BV 100 (Newport Research Corporation) equipped with a stainless steel disc with a rectangular slit ($16 \text{ mm} \times 200 \mu\text{m}$), was employed, in order to reduce the absorption line width with respect to a circular nozzle. In the measurements reported here, depending on the frequency stability of the specific diode laser, a line width of about 0.001 cm^{-1} FWHM has been achieved. Mixtures of 10% of commercial grade (purity $\geq 98\%$) 1-chloro-1,1-difluoroethane in Ne have been expanded through the pulsed slit valve at a stagnation pressure of 1–2 bar. Ne was used for seeding instead of He, which is commonly used, because it has a lower velocity in the supersonic expansion thus reducing the observed line width, and since it is also more efficiently pumped by the oil diffusion pump. The laser frequency has been tuned by applying a ramp on the laser current with a repetition rate of about 1 kHz and an amplitude of 5–30 mA. The pulsed valve has been synchronized with the

laser scan by taking every n th ($n = 200$ – 500) reference TTL signal from the laser current control unit for triggering the valve driver with a proper delay, using a delay generator (Stanford DG535). The simultaneously measured jet spectrum, a cell spectrum and the etalon trace have been averaged on a digital oscilloscope (LeCroy LT224) and transferred to a personal computer. It has been verified that the averaging process with about 100 averages was not contributing significantly to the line width of the observed absorption lines. Typically about 0.2 cm^{-1} scans were made and overlapping scans were assembled after linearization by using programs written in Labview. The absolute frequency calibration was performed by following a method developed by us [11] based on the comparison with high resolution Fourier transform jet spectra, made available by Prof. Don McNaughton. The calibration accuracy is estimated to be better than 0.0004 cm^{-1} .

3 Results and discussion

HCFC-142b is a near-prolate asymmetric top ($\kappa \approx -0.91$), belongs to the C_s symmetry group and possesses 11 fundamental vibrational modes with A' symmetry (appearing as a/b hybrid bands) and 7 with A'' symmetry (c -type bands).

Ground state molecular constants have been determined for $\text{CH}_3\text{CF}_2^{35}\text{Cl}$ and $\text{CH}_3\text{CF}_2^{37}\text{Cl}$, by Graner and Thomas [19] from microwave spectra and more recently by Alonso *et al.* [20], from Fourier transform microwave (FTMW) and millimeter wave spectra. The same authors [19,20] observed splittings due to internal rotation in the lowest torsional vibrational states.

Several low resolution studies of the infrared [21–24] and Raman spectra [21,22,25] of HCFC-142b have been reported and the assignment of the vibrational modes has been established by harmonic force field calculations [23,26,27]. McNaughton *et al.* [28] recorded high resolution (0.0035 cm^{-1} FWHM) FTIR jet spectra of neat $\text{CH}_3\text{CF}_2\text{Cl}$, and analyzed some fundamental bands ν_5 at 1234.921 cm^{-1} , ν_7 at 905.227 cm^{-1} , ν_{14} at 1192.645 cm^{-1} and ν_{15} at 967.627 cm^{-1} and the combination band $\nu_7 + \nu_{11}$ (1215.238 cm^{-1}). Recently Baskakov *et al.* [29] reported high resolution (0.0023 cm^{-1} FWHM) FTIR spectra of natural $\text{CH}_3\text{CF}_2\text{Cl}$ and monoisotopic $\text{CH}_3\text{CF}_2^{35}\text{Cl}$ (0.0029 cm^{-1}) and obtained a very accurate analysis for the ν_7 and ν_8 fundamentals of both isotopic species (^{35}Cl and ^{37}Cl). Newnham and Ballard [30] determined infrared absorbance cross-sections and integrated band strengths from vapour phase FTIR spectra at several temperatures (203–294 K).

The ν_7 fundamental is a CH_3 rocking mode, with A' symmetry in the C_s point group, corresponding with a a/b hybrid band. From the spectra a prominent a -type band is evident, although weaker b -type transitions can be observed as well. Our diode laser slit jet spectra differ from those previously mentioned [28,29], in having a better resolution (about 0.001 cm^{-1} FWHM) and a superior signal to noise ratio, apart from being much

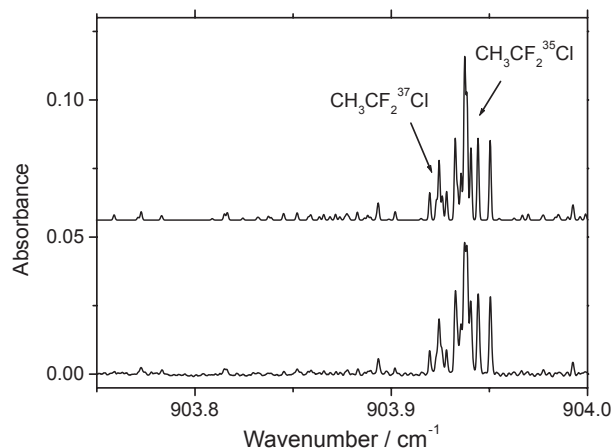


Fig. 2. Detail of the ν_7 band of $\text{CH}_3\text{CF}_2\text{Cl}$. Simulation with a resolution of 0.001 cm^{-1} FWHM for a rotational temperature of 20 K, obtained by using the parameters of Tables 1 and 2. Diode laser slit-jet spectrum for an expansion of 10% of $\text{CH}_3\text{CF}_2\text{Cl}$ through a slit nozzle ($16 \text{ mm} \times 200 \mu\text{m}$). The stronger absorptions are due to a -type transitions of $\text{CH}_3\text{CF}_2^{37}\text{Cl}$ (903.92 – 903.93 cm^{-1}) and $\text{CH}_3\text{CF}_2^{35}\text{Cl}$ (903.93 – 903.95 cm^{-1}), the weaker lines between 903.75 and 903.910 cm^{-1} are b -type transitions. See also Tables 3 and 4 for line assignments.

colder. The rotational temperature in our spectra is estimated to be about 20 K, which has to be compared to the rotational temperature of 50 K determined for the jet expansion reported by reference [28] and the 203 K equilibrium temperature of the cooled cell of reference [29]. This means essentially that we observe fewer transitions, typically with $J \leq 30$ and $K_a \leq 15$, but most of them are well resolved. This implies that transitions of both isotopic species ($\text{CH}_3\text{CF}_2^{35}\text{Cl}$ and $\text{CH}_3\text{CF}_2^{37}\text{Cl}$) could be observed distinctly, without the need for monoisotopic substance.

Note that we did not observe hot-band transitions, which sets an upper limit for the vibrational temperature of about 150 K. Moreover we observed for the first time many weak b -type transitions in the ν_7 spectra, and calculated an approximate intensity ratio between a and b -type dipole transition moments; $\mu_a:\mu_b \approx 1:0.4$. Figure 2 shows the stronger a -type and the weaker b -type transitions for low rotational quantum numbers.

The assignment of the a -type transitions was rather straightforward, and eventually 270 and 159 transitions could be assigned for $\text{CH}_3\text{CF}_2^{35}\text{Cl}$ and $\text{CH}_3\text{CF}_2^{37}\text{Cl}$ respectively. In many cases the absorption of the two isotopic species can be observed distinctly, as can be seen in Figure 3. The search for b -type transitions led to the assignment of 100 resp 24 lines for both isotopic species.

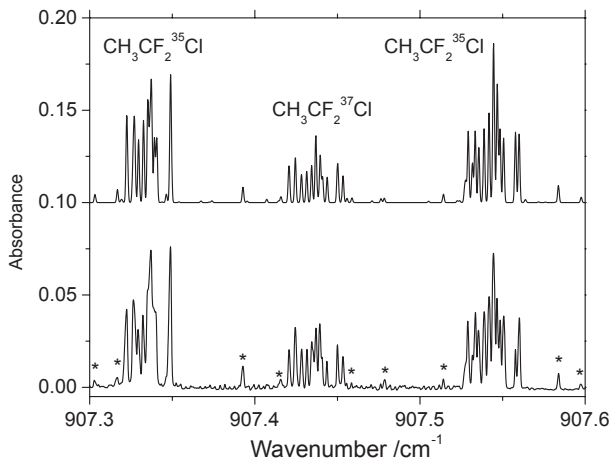
The transitions were fitted to Watson's A-reduced Hamiltonian in the I^r representation, fixing the ground state constants to the values of Alonso *et al.* [20]. Due to the low rotational temperature (about 20 K) only levels with relatively low quantum numbers ($J \leq 30$, $K_a \leq 15$) are sufficiently populated, and the smallest quartic constants could not be determined significantly. By fixing Δ_K ,

Table 1. Molecular constants (in cm^{-1}) for the ν_7 fundamental of $\text{CH}_3\text{CF}_2^{35}\text{Cl}$.

	ground state ^a , reference [20]	ν_7 , reference [28]	ν_7 , reference [29]	ν_7 , [this work]
ν_0		905.227747(54)	905.227626(18)	905.22740(5)
A	0.1747016	0.1741109(30)	0.174292791(62)	0.1742918(6)
B	0.10817162	0.10798(10)	0.107962592(32)	0.1079634(3)
C	0.10523758	0.10511(11)	0.105050246(44)	0.1050496(3)
$\Delta_J/10^{-8}$	1.8221	1.824(33)	1.7547(11)	1.74(3)
$\Delta_{JK}/10^{-8}$	5.8948	10.21(45)	5.5803(35)	6.02(12)
$\Delta_K/10^{-8}$	-3.4563	-90.50(28)	-2.9681(69)	-3.4563 ^a
$\delta_J/10^{-10}$	5.3220	5.3220 ^a	1.258(27)	5.3220 ^a
$\delta_K/10^{-8}$	-1.5223	-1.5223 ^a	-2.780(14)	-1.5223 ^a
fitted lines		465	2003	370
$\sigma/10^{-3}$		0.46	0.35	0.30

^a fixed value**Table 2.** Molecular constants (in cm^{-1}) for the ν_7 fundamental of $\text{CH}_3\text{CF}_2^{37}\text{Cl}$.

	ground state ^a , reference [20]	ν_7 , reference [29]	ν_7 , [this work]
ν_0		904.972349(39)	904.97222(8)
A	0.1746946	0.17428652(30)	0.1742856(14)
B	0.10556532	0.10535496(28)	0.1053577(5)
C	0.10276647	0.10258253(33)	0.1025793(6)
$\Delta_J/10^{-8}$	1.7645	1.783(13)	1.73(5)
$\Delta_{JK}/10^{-8}$	5.7469	5.502(18)	5.83(35)
$\Delta_K/10^{-8}$	-3.2412	-2.925(62)	-3.2412 ^a
$\delta_J/10^{-10}$	4.9961	4.9961 ^a	4.9961 ^a
$\delta_K/10^{-8}$	-1.5451	-1.5451 ^a	-1.5451 ^a
fitted lines		379	187
$\sigma/10^{-3}$		0.29	0.33

^a fixed value**Fig. 3.** Detail of the ν_7 band of $\text{CH}_3\text{CF}_2\text{Cl}$. Upper panel: simulation with a resolution of 0.001 cm^{-1} FWHM for a rotational temperature of 20 K, obtained by using the parameters of Tables 1 and 2. Lower panel: diode laser slit-jet spectrum. Experimental conditions as for Figure 1. The stronger absorptions are due to a -type transitions of $\text{CH}_3\text{CF}_2^{37}\text{Cl}$ $\text{CH}_3\text{CF}_2^{35}\text{Cl}$ ($907.32\text{--}907.35$ and $907.53\text{--}907.56 \text{ cm}^{-1}$) and $\text{CH}_3\text{CF}_2^{37}\text{Cl}$ ($907.415\text{--}907.455 \text{ cm}^{-1}$), the weaker b -type lines are indicated with asterisks. See also Tables 3 and 4 for line assignments.

δ_J and δ_K to the ground state values, a satisfactory fit of all lines could be obtained, yielding accurate molecular constants for both isotopic species ($\text{CH}_3\text{CF}_2^{35}\text{Cl}$ and $\text{CH}_3\text{CF}_2^{37}\text{Cl}$). The resulting parameters are in excellent agreement with the results of Baskakov *et al.* [29] (see Tabs. 1 and 2). A computer simulation of the spectra, which can be seen in Figures 2 and 3, shows an almost perfect agreement with the observed spectra and accounts for practically all observed lines, indicating that hot-bands and possible combination bands, falling in this spectral range give a negligible contribution to the spectra. Tables 3 and 4 report the assignment of all transitions shown in Figures 2 and 3, for $\text{CH}_3\text{CF}_2^{35}\text{Cl}$ and $\text{CH}_3\text{CF}_2^{37}\text{Cl}$ respectively. A complete list with all observed and fitted transitions is available from the authors.

For $\text{CH}_3\text{CF}_2^{35}\text{Cl}$ small perturbations have been observed transitions with $K_a = 14$ and 15 and $J \leq 20$ and with $K_a = 13\text{--}16$ and $J \geq 21$, which agrees rather well with the observations of reference [29]. These perturbed transitions have not been included in the fit.

4 Conclusions

It has been demonstrated that the diode laser slit-jet technique is suitable for the spectroscopic investigation

Table 3. Selected ν_7 transitions of $\text{CH}_3\text{CF}_2^{35}\text{Cl}$ (in cm^{-1}).

$J' K'_a K'_c$	$JK_a K_c$	$\tilde{\nu}_0^{\text{exp}}$	Δ	$J' K'_a K'_c$	$JK_a K_c$	$\tilde{\nu}_0^{\text{exp}}$	Δ	$J' K'_a K'_c$	$JK_a K_c$	$\tilde{\nu}_0^{\text{exp}}$	Δ
6 1 6	7 0 7	903.7725	-1	5 2 4	6 2 5	903.9405	-1	9 3 6	8 2 7	907.4761	-2
4 2 3	5 3 2	903.8148	-1	5 0 5	6 0 6	903.9443	0	10 2 9	9 1 8	907.4786	3
19 9 11	19 10 10	903.8453	4	5 1 5	6 1 6	903.9505	0	11 0 11	10 1 10	907.5141	-1
19 9 10	19 10 9	903.8453	4	20 8 13	20 9 12	903.9774	-1	11 1 11	10 1 10	907.5289	-2
18 9 10	18 10 9	903.8521	0	20 8 12	20 9 11	903.9774	-1	11 9 2	10 9 1	907.5317	-1
18 9 9	18 10 8	903.8521	0	18 8 11	18 9 10	903.9925	3	11 9 3	10 9 2	907.5317	-1
17 9 8	17 10 7	903.8591	1	18 8 10	18 9 9	903.9925	3	11 0 11	10 0 10	907.5335	2
17 9 9	17 10 8	903.8591	1	10 0 10	9 1 9	907.3027	-4	11 8 3	10 8 2	907.5353	-2
16 9 8	16 10 7	903.8657	2	7 5 2	6 4 3	907.3165	-3	11 8 4	10 8 3	907.5353	-2
16 9 7	16 10 6	903.8657	2	7 5 3	6 4 2	907.3165	-3	11 7 4	10 7 3	907.5389	1
15 9 6	15 10 5	903.8719	2	10 1 10	9 1 9	907.3224	1	11 7 5	10 7 4	907.5389	1
15 9 7	15 10 6	903.8719	2	10 7 3	9 7 2	907.3292	-4	11 6 5	10 6 4	907.5418	1
13 9 4	13 10 3	903.8830	1	10 7 4	9 7 3	907.3292	-4	11 6 6	10 6 5	907.5418	1
13 9 5	13 10 4	903.8830	1	10 6 5	9 6 4	907.3322	-4	11 5 6	10 5 5	907.5444	1
3 3 1	4 4 0	903.8934	-1	10 6 4	9 6 3	907.3322	-4	11 5 7	10 5 6	907.5444	1
3 3 0	4 4 1	903.8934	-1	10 5 6	9 5 5	907.3351	0	11 4 7	10 4 6	907.5466	-2
5 0 5	6 1 6	903.9019	0	10 5 5	9 5 4	907.3351	0	11 4 8	10 4 7	907.5466	-1
5 1 4	6 1 5	903.9327	0	10 4 6	9 4 5	907.3370	-4	11 3 9	10 3 8	907.5485	1
5 5 1	6 5 2	903.9356	0	10 4 7	9 4 6	907.3370	-4	11 3 8	10 3 7	907.5507	1
5 5 0	6 5 1	903.9356	0	10 1 9	9 1 8	907.3489	-2	11 1 10	10 1 9	907.5578	0
5 2 3	6 2 4	903.9374	0	10 2 8	9 2 7	907.3489	1	11 2 9	10 2 8	907.5601	2
5 3 3	6 3 4	903.9384	-2	8 4 5	7 3 4	907.3927	1	7 7 0	6 6 1	907.5839	2
5 3 2	6 3 3	903.9384	-1	8 4 4	7 3 5	907.3927	-3	7 7 1	6 6 0	907.5839	2

$\Delta = o - c$ (observed minus calculated) in 10^{-4} cm^{-1} .

Table 4. Selected ν_7 transitions of $\text{CH}_3\text{CF}_2^{37}\text{Cl}$ (in cm^{-1}).

$J' K'_a K'_c$	$JK_a K_c$	$\tilde{\nu}_0^{\text{exp}}$	Δ	$J' K'_a K'_c$	$JK_a K_c$	$\tilde{\nu}_0^{\text{exp}}$	Δ	$J' K'_a K'_c$	$JK_a K_c$	$\tilde{\nu}_0^{\text{exp}}$	Δ
3 2 2	4 3 1	903.7831	3	8 6 3	7 5 2	907.3927	-1	12 2 11	11 2 10	907.4370	1
15 7 8	15 8 7	903.8576	-2	12 11 2	11 11 1	907.4156	-3	12 5 7	11 5 6	907.4370	-1
15 7 9	15 8 8	903.8576	-2	12 11 1	11 11 0	907.4156	-3	12 5 8	11 5 7	907.4370	-1
13 7 7	13 8 6	903.8688	0	12 1 12	11 1 11	907.4207	-1	12 4 9	11 4 8	907.4393	-2
13 7 6	13 8 5	903.8688	0	12 9 3	11 9 2	907.4244	-1	12 4 8	11 4 7	907.4393	-4
12 7 6	12 8 5	903.8739	1	12 9 4	11 9 3	907.4244	-1	12 3 9	11 3 8	907.4436	-3
12 7 5	12 8 4	903.8739	1	12 0 12	11 0 11	907.4244	-2	12 1 11	11 1 10	907.4500	0
4 1 3	5 1 4	903.9196	-1	12 8 4	11 8 3	907.4283	1	12 2 10	11 2 9	907.4533	-2
4 2 2	5 2 3	903.9244	0	12 8 5	11 8 4	907.4283	1	9 5 4	8 4 5	907.4585	-3
4 3 2	5 3 3	903.9244	-1	12 7 6	11 7 5	907.4315	0	9 5 5	8 4 4	907.4585	-3
4 3 1	5 3 2	903.9244	-1	12 7 5	11 7 4	907.4315	0	9 6 3	8 5 4	907.5973	-3
4 0 4	5 0 5	903.9281	-2	12 6 7	11 6 6	907.4344	0	9 6 4	8 5 3	907.5973	-3
8 6 2	7 5 3	907.3927	-1	12 6 6	11 6 5	907.4344	0				

$\Delta = o - c$ (observed minus calculated) in 10^{-4} cm^{-1} .

of HCFC's, by providing cold and well resolved infra red absorption spectra. Many transitions could be unambiguously assigned for $\text{CH}_3\text{CF}_2^{35}\text{Cl}$ and $\text{CH}_3\text{CF}_2^{37}\text{Cl}$, without the need for a monoisotopic substance. The results of the vibration-rotational analysis are in excellent agreement with previous works. In addition many weak b -type transitions have been observed and an approximate a/b -type intensity ratio has been determined.

In general, diode laser slit jet spectroscopy has both advantages and drawbacks with respect to cold cell FTIR measurements. First of all, the strong jet cooling eliminates the absorption due to hot-bands more efficiently than a cold cell. The low rotational temperature in a jet limits the observed lines to those with relatively low quantum numbers, which simplifies the spectra enormously, rendering the analysis easier, but it also reduces the

quantity of data, and thus the number of higher order molecular constants which can be determined. In most cases the spectral resolution obtained by diode laser slit-jet spectroscopy is better ($0.0005\text{--}0.001\text{ cm}^{-1}$) than that of the best FTIR instruments (typically $0.001\text{--}0.004\text{ cm}^{-1}$). In the present case the better resolution and the good signal to noise ratio, allowed us to analyze the $\text{CH}_3\text{CF}_2^{37}\text{Cl}$ spectrum in a natural sample and to observe weak *b*-type transitions in the ν_7 band. If one considers heavier molecules (*e.g.* CCl_3F), with more hot-band contributions and smaller rotational constants, the advantages of the diode slit-jet spectra become more important and FTIR measurements become inadequate, for lighter molecules (*e.g.* CH_2Cl_2), the line density is sufficiently low and high resolution FTIR spectra are preferable.

We thank Professor Don McNaughton for providing us with their high resolution FTIR jet spectra, which we used for calibration.

References

1. S.A. Montzka, J.H. Butler, R.C. Myers, T.M. Thompson, T.H. Swanson, A.D. Clarke, L.T. Lock, J.W. Elkins, *Science* **272**, 1318 (1996)
2. M. Prather, C.M. Spivakovsky, *J. Geophys. Res. D* **95**, 18723 (1990)
3. C. Clerbaux, R. Colin, P.C. Simon, C. Granier, *J. Geophys. Res. D* **98**, 10491 (1993)
4. S.A. Montzka, R.C. Myers, J.H. Butler, J.W. Elkins, *Geophys. Res. Lett.* **21**, 2483 (1994)
5. C.B. Farmer, O.F. Raper, F.G. O'Callaghan, Final Report on the First Flight of the ATMOS Instrument During the Spacelab 3 Mission, April 29 through May 6, 1985 JPL Publication 87-32, Jet Propulsion laboratory, California Institute of Technology, Pasadena, CA, 1987
6. R. Zander, C.P. Rinsland, C.B. Farmer, R.H. Norton, *J. Geophys. Res. D* **92**, 9836 (1987)
7. B. Sen, G.C. Toon, J.-F. Blavier, E.L. Fleming, C.H. Jackman, *J. Geophys. Res. D* **101**, 9045 (1996)
8. M. Snels, in *Recent Res. Devel. Mol. Spectroscopy* (Transworld Research Network, Kerala, India, 2002), ISBN 81-7895-026-X
9. M. Snels, A. Beil, H. Hollenstein, M. Quack, U. Schmitt, F. D'Amato, *J. Chem. Phys.* **103**, 8846 (1995)
10. M. Snels, G. D'Amico, L. Piccarreta, H. Hollenstein, M. Quack, *J. Mol. Spectrosc.* **205**, 102 (2001)
11. M. Snels, G. D'Amico, *J. Mol. Spectrosc.* **209**, 1 (2001)
12. M. Snels, G. D'Amico, H. Hollenstein, M. Quack, *Phys. Chem. Chem. Phys.* **4**, 1531 (2002)
13. Z. Wang, M. Eliades, K. Carron, J.W. Bevan, *Rev. Sci. Instrum.* **62**, 21 (1991)
14. K.L. Busarow, G.A. Blake, K.B. Laughlin, R.C. Cohen, Y.T. Lee, R.J. Saykally, *J. Chem. Phys.* **89**, 1268 (1988)
15. C.M. Lovejoy, D.J. Nesbitt, *Rev. Sci. Instrum.* **58**, 807 (1987)
16. A. De Piante, E.J. Campbell, S.J. Buelow, *Rev. Sci. Instrum.* **60**, 858 (1989)
17. T.A. Hu, E.L. Chappell, J.T. Munley, S.W. Sharpe, *Rev. Sci. Instrum.* **64**, 3380 (1993)
18. K. Liu, R.S. Fellers, M.R. Viant, R.P. McLaughlin, M.G. Brown, R.J. Saykally, *Rev. Sci. Instrum.* **67**, 410 (1996)
19. G. Graner, C. Thomas, *J. Chem. Phys.* **49**, 4160 (1968)
20. J.L. Alonso, J.C. López, S. Blanco, A. Guarnieri, *J. Mol. Spectrosc.* **182**, 148 (1997)
21. D.C. Smith, G.M. Brown, J.R. Nielsen, R.M. Smith, Y. Liang, *J. Chem. Phys.* **20**, 473 (1952)
22. J.R. Durig, S.M. Craven, C.W. Hawley, J. Bragin, *J. Chem. Phys.* **57**, 131 (1972)
23. T. Sakka, Y. Ogata, M. Iwasaki, *J. Phys. Chem.* **96**, 10697 (1992)
24. F.B. Brown, A.D.H. Clague, N.D. Heitkamp, D.P. Koster, A. Danti, *J. Mol. Spectrosc.* **24**, 163 (1967)
25. A. Melchior, I. Bar, S. Rosenwaks, *J. Phys. Chem. A* **102**, 7273 (1998)
26. S. Papasavva, K.H. Illinger, J.E. Kenny, *J. Mol. Struct. (Theochem)* **393**, 73 (1997)
27. G.M. Kuramshina, F. Weinhold, Yu.A. Pentin, *J. Chem. Phys.* **109**, 7286 (1998)
28. D. McNaughton, C. Evans, *J. Mol. Spectrosc.* **182**, 342 (1997)
29. O.I. Baskakov, V.V. Ilyushin, E.A. Alekseev, H. Bürger, G. Pawelke, *J. Mol. Spectrosc.* **202**, 285 (2000)
30. D. Newnham, J. Ballard, *J. Quant. Spectrosc. Radiat. Transfer* **53**, 471 (1995)